Synthesis, Reactions, and Nuclear Magnetic Resonance Studies of Some Substituted *arachno*-Decaborane and *arachno*-Nonaborane Derivatives, and the Isolation of Novel Polyhedral Diplatinaboranes. Crystal and Molecular Structure of $[Pt_2(PMe_2Ph)_2(\eta^3\text{-}B_2H_5)(\eta^3\text{-}B_6H_9)]$ *

Rohana Ahmad, Janet E. Crook, Norman N. Greenwood, and John D. Kennedy
Department of Inorganic and Structural Chemistry, University of Leeds, Leeds LS2 9JT

Reaction of *nido*-2-$XB_{10}H_{13}$ (X = Cl, Br, or I) with SMe_2 afforded almost quantitative yields of *arachno*-2-X-6,9-$(SMe_2)_2$-$B_{10}H_{11}$ which, when heated under reflux with ROH (R = Me or Et), gave moderate yields of *arachno*-1-X-4-(SMe_2)-B_9H_{12} together with the corresponding *arachno*-4-(SMe_2)-7-(OR)-B_9H_{12}. Deprotonation of 1-Cl-4-(SMe_2)-B_9H_{12} followed by reaction with *cis*-$[PtCl_2(PMe_2Ph)_2]$ gave [2-Cl-4,4-$(PMe_2Ph)_2$-*arachno*-4-PtB_8H_{11}]. Similar treatment of 4-(SMe_2)-7-(OMe)-B_9H_{12} gave the corresponding compound [8-(OMe)-4,4-$(PMe_2Ph)_2$-*arachno*-4-PtB_8H_{11}] together with variable (small) yields of the known $[(PMe_2Ph)_2PtB_3H_7]$ and [*conjuncto*-$Pt_2(PMe_2Ph)_2(B_6H_9)_2$], the novel, yellow, air-stable crystalline compound [*conjuncto*-$Pt_2(PMe_2Ph)_2(B_2H_5)(B_6H_9)$], and a new, green, air-stable compound tentatively formulated as [*closo*-$(PMe_2Ph)_3Pt_2B_9H_8(OMe)$]. Single-crystal *X*-ray diffraction studies on [*conjuncto*-$Pt_2(PMe_2Ph)_2(B_2H_5)(B_6H_9)$], together with its n.m.r. properties, revealed a novel cluster geometry in which the central almost-linear P–Pt–Pt–P unit is co-ordinated by an η^3-B_6H_9 *nido*-subcluster and an opposing η^3-B_2H_5 moiety. The crystals are monoclinic, space group $P2_1$, with a = 1 618.3(9), b = 1 330.0(7), c = 592.3(3) pm, β = 93.62(4)°, and Z = 2. Detailed ^1H, ^{11}B, and ^{31}P n.m.r. studies of the various halogen- and alkoxy-substituted platinaboranes are presented, and the mechanistic implications of the observed positions of substitution in the products are discussed.

The *arachno*-bis(ligand)decaboranes, $L_2B_{10}H_{12}$, are a well characterized group of borane adducts whose reactions have been studied for many years.[1–3] Boron-substituted derivatives of these adducts are less well known though 2-Br-6,9-$L_2B_{10}H_{11}$ (L = MeCN, PPh_3, or SEt_2)[4] and 5-Br-6,9-$(SMe_2)_2$-$B_{10}H_{11}$[5] have been reported. Likewise, the parent *arachno*-nonaborane species LB_9H_{13} and $[B_9H_{14}]^-$ are well known but boron-substituted derivatives are sparse, *e.g.* 4-(SMe_2)-6-Br-B_9H_{12} and 4-(SMe_2)-6-(OMe)-B_9H_{12}.[5] We are now using a selection of such derivatives in the study of details of skeletal degradations, expansions, or rearrangements which might occur during the synthesis of metallaborane cluster compounds. Initially the four-co-ordinate platinum(II) compound *cis*-$[PtCl_2(PMe_2Ph)_2]$ has been used as the metal-containing reagent, and several of the reactions, which we report here, are shown to be unexpectedly complex: in addition to cluster rearrangements and partial degradations some novel dimetalla species are formed. The crystal and molecular structure of one of these, the *conjuncto*-diplatinadecaborane $[Pt_2(PMe_2Ph)_2(\eta^3\text{-}B_2H_5)(\eta^3\text{-}B_6H_9)]$ (containing a Pt–Pt bond), has been briefly reported in a preliminary communication.[6] The cluster geometry and I.U.P.A.C.-recommended numbering scheme for the parent *arachno*-adducts $L_2B_{10}H_{12}$ and LB_9H_{13} are shown in structures (**1**) and (**2**) in which open circles represent BH. The structure and numbering of the *nido* nine-vertex structure of $[3\text{-}ClB_9H_{11}]^-$, also used in this work, is shown in structure (**3**), where B(3) bears a Cl substituent, and no H atom.

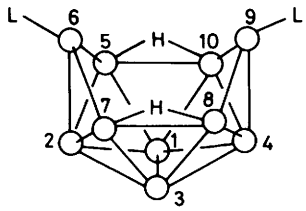

(1)

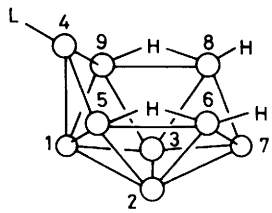

(2)

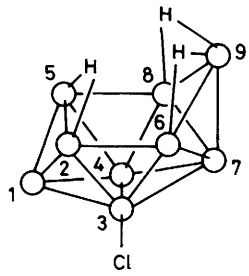

(3)

Results and Discussion

Synthesis of B-*Substituted Borane Derivatives.*—Using a modification of published procedures[4,5] monohalogenated bis(ligand)-*arachno*-decaboranes were prepared by allowing 2-$XB_{10}H_{13}$ (X = Cl, Br, or I) to react with dimethyl sulphide under nitrogen at room temperature for 8 h: equation (1). The

$$2\text{-}XB_{10}H_{13} + 2\,SMe_2 \longrightarrow 2\text{-X-6,9-}(SMe_2)_2\text{-}B_{10}H_{11} + H_2 \quad (1)$$

products were obtained as white crystalline solids in 85—93% yield. The corresponding nonaborane mono-adducts were then

* μ-[Nonahydrohexaborato-$B^2(Pt^1)$,$B^3(Pt^{1,2})$,$B^4(Pt^2)$]-μ-[pentahydrodiborato-$B^1(Pt^{1,2})$,$B^2(Pt^2)$]-bis[(dimethylphenylphosphine)platinum](*Pt–Pt*).

Supplementary data available (No. SUP 56620, 3 pp.): thermal parameters, see Instructions for Authors, *J. Chem. Soc., Dalton Trans.*, 1986, Issue 1, pp. xvii—xx. Structure factors are available from the editorial office.

made by heating these freshly prepared decaborane bis-adducts in methanol (or ethanol) under reflux: equation (2). The

$$2\text{-X-6,9-}(SMe_2)_2\text{-}B_{10}H_{11} \xrightarrow[\text{reflux}]{ROH} 1\text{-X-4-}(SMe_2)\text{-}B_9H_{12} + B(OR)_3 + SMe_2 + H_2 \quad (2)$$

products were obtained as colourless crystals in 15—20% yield after separation by column chromatography from unreacted material and from the alkoxide coproducts 4-(SMe_2)-7-(OR)-B_9H_{12} (R = Me or Et) which were obtained as colourless needles in 20—30% yield: equation (3).

$$2\text{-X-6,9-}(SMe_2)_2\text{-}B_{10}H_{11} \xrightarrow[\text{reflux}]{ROH} 4\text{-}(SMe_2)\text{-7-(OR)-}B_9H_{12} + B(OR)_3 + SMe_2 + HX + H_2 \quad (3)$$

Reactions with cis-$[PtCl_2(PMe_2Ph)_2]$.—Treatment of 1-Cl-4-(SMe_2)-B_9H_{12} (**4**) with a 'proton sponge', *i.e.* 1,8-bis(dimethylamino)naphthalene, and *cis*-$[PtCl_2(PMe_2Ph)_2]$ in the mole ratios 1:2:1 afforded [2-Cl-4,4-$(PMe_2Ph)_2$-4-PtB_8H_{11}] (**5**) in 30% yield: equation (4).

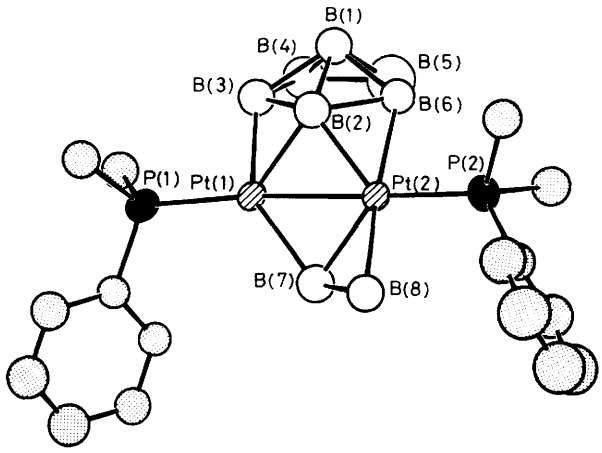

Figure 1. ORTEP drawing of the molecular structure of $[Pt_2(PMe_2Ph)_2(\eta^3\text{-}B_2H_5)(\eta^3\text{-}B_6H_9)]$. Hydrogen atoms were not located in the diffraction analysis but are reasonably inferred from n.m.r. spectroscopy (see text)

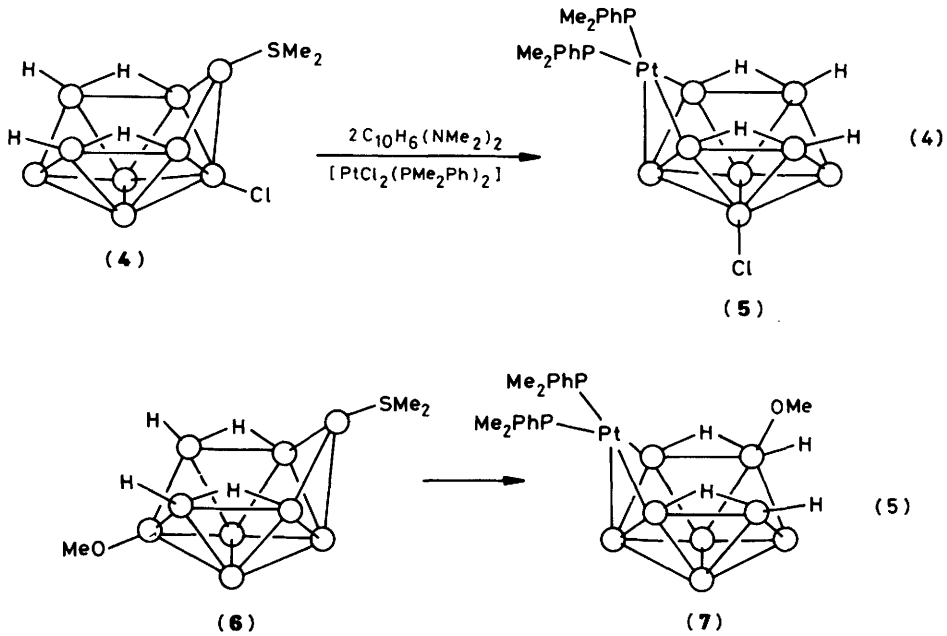

Compound (**5**) may also be obtained in 75% yield from the reaction between the *nido*-anion $[3\text{-Cl-}B_9H_{11}]^-$ (**3**) and $[PtCl_2(PMe_2Ph)_2]$ in methanol solution. The n.m.r. evidence for this structural assignment and its mechanistic implications are considered below.

Similar treatment of the methoxy derivative 4-(SMe_2)-7-(OMe)-B_9H_{12} (**6**) with 2 mol equiv. of proton sponge and 1 mol equiv. of *cis*-$[PtCl_2(PMe_2Ph)_2]$ gave several products of which the predominant one was [8-(OMe)-4,4-$(PMe_2Ph)_2$-4-PtB_8H_{11}] (**7**): equation (5). In addition several skeletal degradation products were identified although not in consistent yields. These include the known compounds $[(PMe_2Ph)_2PtB_3H_7]$[7] (8% yield) and $[Pt_2(PMe_2Ph)_2(\eta^3\text{-}B_6H_9)_2]$[8,9] (35% yield), the novel, yellow, air-stable crystalline compound $[Pt_2(PMe_2Ph)_2(\eta^3\text{-}B_2H_5)(\eta^3\text{-}B_6H_9)]$ (*Pt–Pt*) (2—3% yield) and a new, green, air-stable compound tentatively formulated as a *closo*-diplatinaundecaborane $[(PMe_2Ph)_3Pt_2B_9H_8(OMe)]$ (2—3% yield) (see below). The yields quoted are the maximum ones observed on particular occasions.

The compounds were separated by thin-layer chromatography, although this did not result in the mutual separation of $[(PMe_2Ph)_2PtB_3H_7]$ from $[Pt_2(PMe_2Ph)_2(B_2H_5)(B_6H_9)]$, which were always obtained as mixtures. However, heating of these mixtures in dichloromethane solution resulted in the selective decomposition of the thermally less robust[7] PtB_3H_7 species and thence permitted the isolation of pure $[Pt_2(PMe_2Ph)_2(B_2H_5)(B_6H_9)]$ by further chromatography.

Crystal and Molecular Structure of $[Pt_2(PMe_2Ph)_2(\eta^3\text{-}B_2H_5)(\eta^3\text{-}B_6H_9)]$.—An ORTEP drawing of the molecular structure showing the numbering system used is presented in Figure 1 and selected interatomic distances and angles are in Tables 1 and 2. The structure consists of a four-vertex Pt_2B_2 and an eight-vertex Pt_2B_6 subcluster conjoined at a common Pt–Pt edge. It is therefore quite different from the previously characterized 'isoelectronic' *arachno*-diplatinadecaborane [6,6,9,9-$(PMe_2Ph)_4$-6,9-$Pt_2B_8H_{10}$][10] which geometrically closely resembles the icosahedral fragment *arachno*-$[B_{10}H_{14}]^{2-}$ with the

6,9-positions subrogated by the $Pt(PMe_2Ph)_2$ groups. The Pt–Pt interatomic distance (262.1 pm) is similar to that in $[Pt_2(PMe_2Ph)_2(\eta^3\text{-}B_6H_9)_2]$ (264.3 pm)[8,9] and is also typical for many Pt–Pt bonds in bridged organometallic compounds.[11] There is an essentially linear P–Pt–Pt–P axis to which the B_6 and B_2 subclusters are appended: P(1)–Pt(1)–Pt(2) 174.8, P(2)–Pt(2)–Pt(1) 178.3°. The four atoms B(2), Pt(1), Pt(2), and B(7) are essentially coplanar, the dihedral angle between the Pt(1)Pt(2)B(2) and Pt(1)Pt(2)B(7) planes being 0.9°. The hydrogen atoms were not locatable from the *X*-ray diffraction analysis because of the limited quality of the data set, but n.m.r. studies (see below) suggest that there are nine hydrogen atoms associated with the B_6 subcluster and five hydrogen atoms associated with the B_2 subcluster. Indeed, the η^3-B_6H_9 moiety bridges the Pt–Pt unit in exactly the same way as previously

Table 1. Interatomic distances (pm) for $[Pt_2(PMe_2Ph)_2(\eta^3\text{-}B_2H_5)(\eta^3\text{-}B_6H_9)]$ with estimated standard deviations in parentheses

(a) From the platinum atoms			
Pt(1)–Pt(2)	262.1(1)	Pt(2)–P(2)	229.2(5)
Pt(1)–P(1)	228.8(5)	Pt(2)–B(2)	219.3(24)
Pt(1)–B(2)	218.1(23)	Pt(2)–B(6)	227.7(24)
Pt(1)–B(3)	217.4(25)	Pt(2)–B(7)	215.8(26)
Pt(1)–B(7)	222.4(28)	Pt(2)–B(8)	224.4(26)
(b) Boron–boron		*(c)* Phosphorus–carbon	
B(1)–B(2)	189.2(34)	P(1)–C(11)	182.9(10)
B(1)–B(3)	189.3(32)	P(1)–C(Me11)	185.6(21)
B(1)–B(4)	179.2(37)	P(1)–C(Me12)	183.4(23)
B(1)–B(5)	170.7(37)	P(2)–C(21)	182.5(13)
B(1)–B(6)	177.7(37)	P(2)–C(Me21)	184.7(22)
B(2)–B(3)	178.8(34)	P(2)–C(Me22)	187.4(20)
B(2)–B(6)	183.0(30)		
B(3)–B(4)	185.3(34)		
B(4)–B(5)	176.0(42)		
B(5)–B(6)	180.9(38)		
B(7)–B(8)	186.9(37)		

Table 2. Angles (°) between interatomic vectors for $[Pt_2(PMe_2Ph)_2(\eta^3\text{-}B_2H_5)(\eta^3\text{-}B_6H_9)]$ with estimated standard deviations in parentheses

(a) At the platinum atoms		*(b)* Boron–boron–platinum	
P(1)–Pt(1)–Pt(2)	174.8(1)	B(1)–B(2)–Pt(1)	121.0(14)
B(2)–Pt(1)–Pt(2)	53.4(6)	B(1)–B(2)–Pt(2)	122.5(13)
B(3)–Pt(1)–Pt(2)	96.3(6)	B(3)–B(2)–Pt(1)	65.5(11)
B(7)–Pt(1)–Pt(2)	52.1(7)	B(3)–B(2)–Pt(2)	128.1(14)
P(2)–Pt(2)–Pt(1)	178.3(1)	B(6)–B(2)–Pt(1)	121.7(13)
B(2)–Pt(2)–Pt(1)	53.0(6)	B(6)–B(2)–Pt(2)	68.3(11)
B(6)–Pt(2)–Pt(1)	91.2(6)	B(1)–B(3)–Pt(1)	121.3(15)
B(7)–Pt(2)–Pt(1)	54.4(7)	B(2)–B(3)–Pt(1)	66.0(11)
B(8)–Pt(2)–Pt(1)	94.5(6)	B(4)–B(3)–Pt(1)	122.0(15)
Pt(2)–B(2)–Pt(1)	73.6(7)	B(1)–B(6)–Pt(2)	123.8(14)
Pt(2)–B(7)–Pt(1)	73.5(9)	B(2)–B(6)–Pt(2)	63.5(10)
B(2)–Pt(1)–P(1)	131.0(6)	B(5)–B(6)–Pt(2)	127.8(15)
B(3)–Pt(1)–P(1)	88.9(7)	B(8)–B(7)–Pt(1)	121.9(15)
B(7)–Pt(1)–P(1)	123.4(7)	B(8)–B(7)–Pt(2)	67.3(11)
B(2)–Pt(2)–P(2)	125.5(6)	B(7)–B(8)–Pt(2)	62.5(11)
B(6)–Pt(2)–P(2)	88.0(6)		
B(7)–Pt(2)–P(2)	127.1(8)	*(c)* Boron–boron–boron	
B(8)–Pt(2)–P(2)	86.3(6)	Range 56.4—63.3, mean 60.0	
B(3)–Pt(1)–B(2)	48.5(9)	Range 105.6—110.0, mean 107.8	
B(7)–Pt(1)–B(2)	105.5(9)		
B(7)–Pt(1)–B(3)	141.3(9)	*(d)* Carbon–phosphorus–platinum	
B(6)–Pt(2)–B(2)	48.3(8)	C(Me11)–P(1)–Pt(1)	113.8(7)
B(7)–Pt(2)–B(2)	107.4(10)	C(Me12)–P(1)–Pt(1)	116.9(7)
B(7)–Pt(2)–B(6)	134.4(10)	C(11)–P(1)–Pt(1)	113.3(5)
B(8)–Pt(2)–B(2)	136.3(8)	C(Me21)–P(2)–Pt(2)	112.9(7)
B(8)–Pt(2)–B(6)	174.3(9)	C(Me22)–P(2)–Pt(2)	115.3(7)
B(8)–Pt(2)–B(7)	50.2(9)	C(21)–P(2)–Pt(2)	120.9(6)

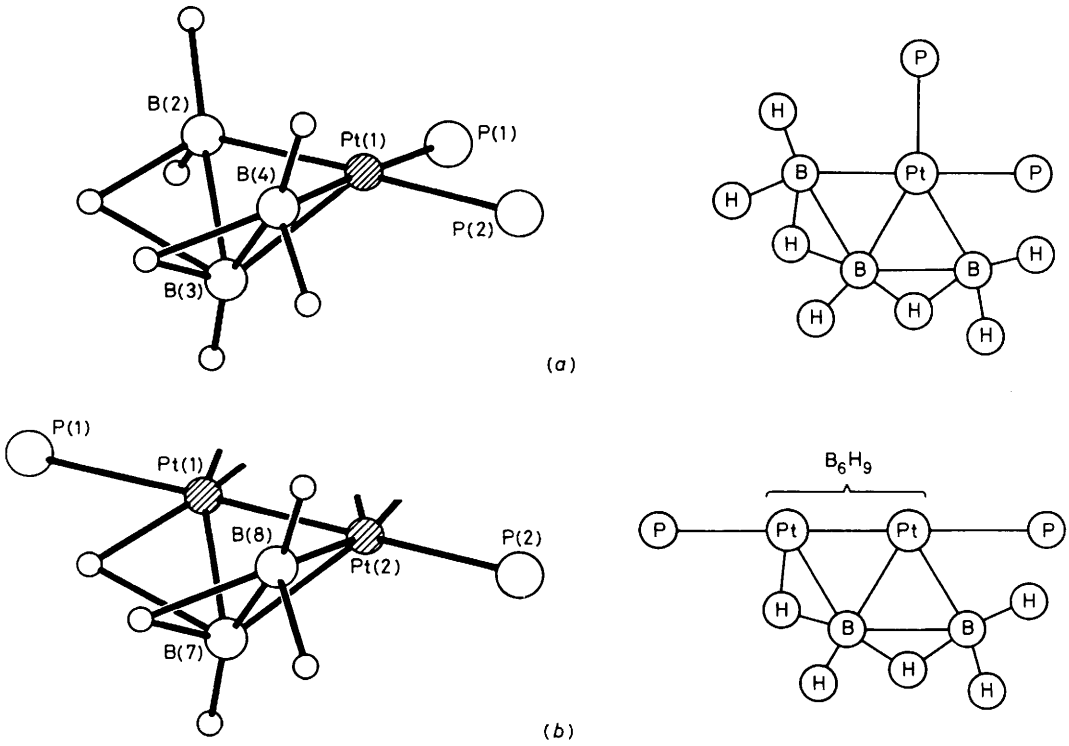

Figure 2. Schematic representation of the disposition of hydrogen atoms in *(a)* $[(PMe_2Ph)_2PtB_3H_7]$ and *(b)* the $Pt_2(B_2H_5)$ moiety in $[Pt_2(PMe_2Ph)_2(B_2H_5)(B_6H_9)]$

Table 3. Selected n.m.r. parameters in substituted *arachno* nine-vertex platinanonaboranes [4,4-$(PMe_2Ph)_2$-4-$PtB_8H_{11}X$] (in $CDCl_3$ solution at +21 °C unless otherwise specified)

	X = H[b,c]		X = 8-(OMe)[d,e]	X = 2-Cl[d,f]	
Assignment[a]	δ(^{11}B)[g]	δ(^{1}H)[h,i]	δ(^{11}B)[g]	δ(^{11}B)[g]	δ(^{1}H)[h,j]
2	−31.6	+0.92[k]	−32.7	−11.8[l]	—
3	−31.6	+0.92[k]	−26.5	−33.2	+1.21
6	−23.0	+2.12, +0.25	−18.9	−19.6	+2.37, +0.03
8	−23.0	+2.12, +0.25	+6.3[l]	−23.7	+2.29, +0.82
5	+1.7[m]	+2.97[n]	*ca.* −7.0[m]	−3.1[m]	+2.91
9	+1.7[m]	+2.97[n]	*ca.* −6.0[m]	−1.2[o]	+3.32
7	+18.8	+4.20	+16.0	+17.6	+4.45
1	+21.6[p]	+3.97	+20.8	+21.7[q]	+4.00
5,6		−3.05[r]			−2.03[s]
8,9		−3.05[r]			−2.79[t]

[a] For numbering see structure (**2**). [b] Data from ref. 10. [c] δ(^{31}P) = −6.7 p.p.m. with $^1J(^{195}Pt–^{31}P)$ 2 724 Hz; measured at −60 °C. [d] This work. [e] δ(^{31}P) −5.8 p.p.m. [$^1J(^{195}Pt–^{31}P)$ 2 829 Hz] and −6.4 p.p.m. [$^1J(^{195}Pt–^{31}P)$ 2 707 Hz] with $^2J(^{31}P–^{31}P)$ *ca.* 27 Hz; measured at −48 °C. [f] δ(^{31}P) −6.7 p.p.m. [$^1J(^{195}Pt–^{31}P)$ 2 818 Hz] and −7.7 p.p.m. [$^1J(^{195}Pt–^{31}P)$ 2 667 Hz] with $^2J(^{31}P–^{31}P)$ *ca.* 25 Hz; measured at −45 °C. [g] δ(^{11}B) in p.p.m. (±1.0) to high frequency (low field) of Ξ 32 083 971 Hz [$BF_3(OEt_2)$]. All ^{11}B resonances are doublets arising from couplings $^1J(^{11}B–^1H)$ except where indicated (see footnote *l*). [h] δ(^{1}H) in p.p.m. (±0.05) to high frequency (low field) of $SiMe_4$; ^{1}H resonances assigned to directly bound B positions by selective ^{1}H-{^{11}B} spectroscopy. [i] δ(^{1}H) (PMe_2) +1.75 and +1.67 p.p.m. with $^3J(^{195}Pt–^1H)$ 27.3 and 25.6, $^2J(^{31}P–^1H)$ 8.5 and 8.3 Hz respectively. [j] δ(^{1}H) (PMe_2) +1.79, +1.72, +1.69, and +1.61 p.p.m. with $^3J(^{195}Pt–^1H)$ 28.6, 26.9, 26.6, and 25.9 Hz respectively. [k] $^nJ(^{195}Pt–^1H)$ 62 Hz. [l] Singlet resonance; point of attachment of substituent X. [m] $^1J(^{195}Pt–^{11}B)$ *ca.* 260 Hz. [n] $^2J(^{195}Pt–^1H)$ *ca.* 30 Hz. [o] $^1J(^{195}Pt–^{31}P)$ *ca.* 280 Hz. [p] $^1J(^{195}Pt–^{31}P)$ *ca.* 330 Hz. [q] $^1J(^{195}Pt–^{31}P)$ *ca.* 340 Hz. [r] $^2J(^{195}Pt–^1H)$ 43 Hz. [s] $^2J(^{195}Pt–^1H)$ *ca.* 50 Hz. [t] $^2J(^{195}Pt–^1H)$ *ca.* 40 Hz.

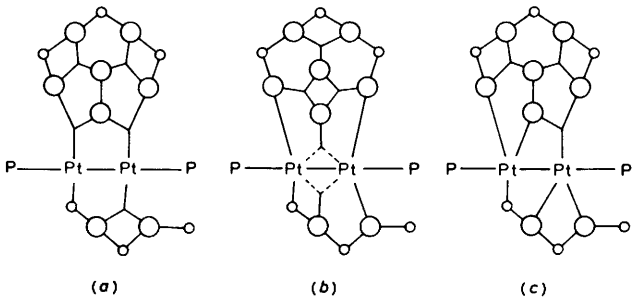

Figure 3. Possible valence-bond descriptions of the bonding in $[Pt_2(PMe_2Ph)_2(\eta^3\text{-}B_2H_5)(\eta^3\text{-}B_6H_9)]$. Each large circle represents BH and the small circles represent bridging hydrogen atoms H_μ or the supernumerary terminal hydrogen atom H_t in the BH_2 group

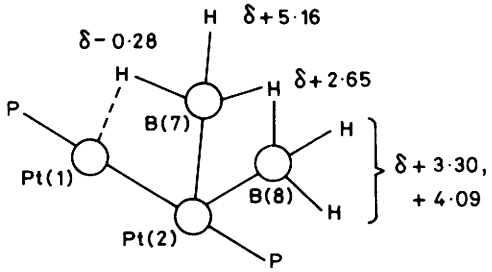

(**8**)

found for $[Pt_2(PMe_2Ph)_2(\eta^3\text{-}B_6H_9)_2]$.[8,9] The B_2H_5 subcluster, however, is without precedent. The nature of the n.m.r. behaviour [see structure (**8**)], together with its correspondence with those of other *arachno*-four-vertex cluster species such as $[(PMe_2Ph)_2PtB_3H_7)]$ [Figure 2(*a*)], $[Ir(PPh_3)_2(CO)H\text{-}(B_3H_7)]$, and $[Ir(PPh_3)_2H_2(B_3H_8)]$, indicates that the disposition of the hydrogen atoms is as depicted in Figure 2(*b*).

A simple valence-bond rationale for the entire ten-vertex cluster structure can thus be written down on the basis of bidentate ligation of both η^3-*nido*-$[B_6H_9]^-$ and η^3-*nido*-$[B_2H_5]^-$ to the central linear bimetallic system P–Pt–Pt–P as shown in Figure 3(*a*). Such a scheme facilitates electron 'book-keeping' but is clearly on oversimplification and there is presumably some admixture of contributions from configurations such as those in Figure 3(*b*) and (*c*). These conclusions are consistent with the results of n.m.r. spectroscopy as discussed in the following section.

N.M.R. Spectroscopy.—(*i*) *The 2-halogenated ten-vertex* arachno-*decaboranes* 2-X-6,9-$(SMe_2)_2$-$B_{10}H_{11}$, *where* X = Cl, Br, *or* I *and the substituted nine-vertex* arachno-*nonaboranes* 7-(OMe)-4-(SMe_2)-B_9H_{12} *and* 1-X-4-(SMe_2)-B_9H_{12}, *where* X = Cl *or* Br. The measured n.m.r. parameters for these species are summarized in the Experimental section and are entirely consistent with their formulations; in particular the similarities to their unsubstituted parents $(SMe_2)B_9H_{13}$ and $(SMe_2)_2$-$B_{10}H_{12}$ are apparent, with the α, β, γ, and δ substituent effects upon halogenation being within, although at the lower end of, previously established ranges.[5,12–19] The α-effect of the methoxy group in 7-(OMe)-4-(SMe_2)-B_9H_{12}, however, is larger (Δσ −20 p.p.m.) and is now bigger, for example, than the α-effect reported for hydroxy substitution in 6-(OH)-$B_{10}H_{13}$ in the *nido*-decaboranyl system, illustrating the marked difference in α-substituent effect that can occur as the site of the substituent is varied. There are also correspondingly larger changes in the β, γ, and δ effects for this methoxy compound, with Δσ for these ranging from −2.0 to +4.3 p.p.m.

(*ii*) *The substituted nine-vertex* arachno-4-*platinanonaboranes* $[2\text{-Cl-}4,4\text{-}(PMe_2Ph)_2\text{-}4\text{-}PtB_8H_{11}]$ *and* $[8\text{-(OMe)-}4,4\text{-}(PMe_2Ph)_2\text{-}4\text{-}PtB_8H_{11}]$. It can be seen that the overall ^{1}H, ^{11}B, and ^{31}P shielding and coupling patterns of the substituted platinanonaboranes are very similar to the parent compound,[10,20] which confirms the overall structural type (Table 3), and that the ^{11}B(2) and ^{11}B(8) positions in the chloro and methoxy compounds respectively are considerably deshielded with respect to the parent, showing these to be the points of substitution: the ^{11}B(2,3) and ^{11}B(5,8) resonances in $[(PMe_2\text{-}Ph)_2PtB_8H_{12}]$ occur at highest field and are well distinguished; it is therefore clear that it is components from these two positions that exhibit the lower shielding expected for electronegative substitution. The overall assignments in Table 3

Table 4. Proton and boron-11 n.m.r. data for the metallaborane cluster atoms in $[Pt_2(PMe_2Ph)_2(B_2H_5)(B_6H_9)]$ (CD_2Cl_2 solution at +21 °C) together with selected data (in parentheses) for $[Pt_2(PMe_2Ph)_2(B_6H_9)_2]$ for comparison

Assignment[a]	$\delta(^{11}B)$/p.p.m.[b,c]	$^1J(^{195}Pt-^{11}B)$/Hz[c] (approx.)	$\delta(^1H)$/p.p.m.[c,d]
1	−42.9 (−42.0)	—	+0.57 (+0.72)
2	+58.7 (+59.7)	330 (330)	+6.53 (+6.00)
3	−7.0 (−3.6)	320 (300)	+3.05 (+3.13)
4	+12.1 (+8.3)	—	+4.20 (+4.13)
5	+6.9 (+8.3)	—	+3.90 (+4.13)
6	−3.7 (−3.6)	300 (300)	+3.13 (+3.13)
7	+52.9	240, 560	+5.16
8	−2.4	330	+4.09
			+3.30
bridge (B_2H_5 unit)	—	—	+2.65
			−0.28
bridge (B_6H_9 unit)	—	—	−1.04 (−1.01)
			−1.22 (−1.01)
			−1.42 (−1.14)

[a] Numbering as in Figure 1; note that the numbering used for the B_6H_9 subcluster differs from that used in refs. 8 and 9; for discussion of assignments see text. [b] $\delta(^{11}B)$ ±0.5 p.p.m. to high frequency (low field) of Ξ 32 083 971 Hz $[BF_3(OEt_2)]$.[15] All ^{11}B resonances are broad doublets with splittings $^1J(^{11}B-^1H)$. [c] Corresponding values for $[Pt_2(PMe_2Ph)_2(B_6H_9)_2]$ (data from ref. 9) in parentheses. [d] $\delta(^1H)$ ±0.05 p.p.m. to high frequency (low field) of internal $SiMe_4$; ^1H resonances related to directly bound boron positions by selective $^1H-\{^{11}B\}$ spectroscopy; see p. 2338.

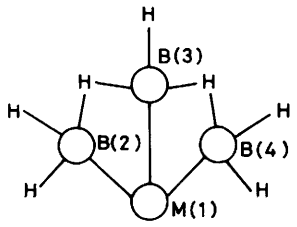

(9)

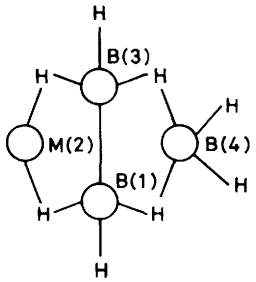

(10)

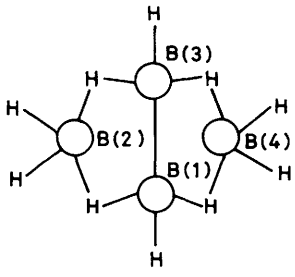

(11)

are also consistent with the small non-α shielding effects thereby derived, with the incidence of couplings $^1J(^{195}Pt-^{11}B)$, with the results of $^1H-\{^{11}B(selective)\}$ spectroscopy, and with the linewidths in the ^{11}B spectra which vary significantly with site position in this particular cluster type (*e.g.* Figure 3 in ref. 10). The α-deshielding effect of the chlorine atom on B(2) is now *ca.* +19 p.p.m., much larger than for the unplatinated nine- and ten-vertex *arachno* clusters, again illustrating how this can vary with substituent position and cluster type, and the 8-methoxy deshielding effect (Δσ −29.3 p.p.m.) is also much larger than that at B(7) in 7-(OMe)-4-(SMe_2)-B_9H_{12}.

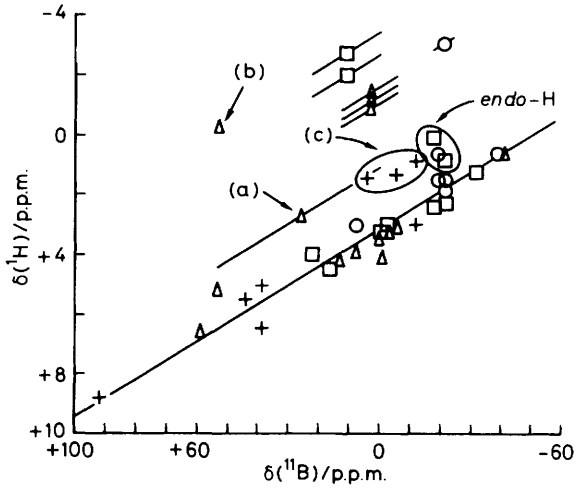

Figure 4. Plot of $\delta(^1H)$ *versus* $\delta(^{11}B)$ for compounds reported in this work: 7-(OEt)-4-(SMe_2)-B_9H_{12} (○), [2-Cl-4,4-$(PMe_2Ph)_2$-4-PtB_8H_{11}] (□), $[Pt_2(PMe_2Ph)_2(B_2H_5)(B_6H_9)]$ (△), and $[(PMe_2Ph)_3Pt_2B_9H_8(OMe)]$ (+). Data (a) and (b) are for bridging H atoms in the B_2H_5 unit of $[Pt_2(PMe_2Ph)_2(B_2H_5)(B_6H_9)]$ (see text). The line drawn has gradient $\delta(^{11}B):\delta(^1H)$ of 16:1 (*cf.* refs. 9 and 19)

(*iii*) *The open* conjuncto *bimetallic cluster compound* $[Pt_2(PMe_2Ph)_2(B_2H_5)(B_6H_9)]$. Consistent with the molecular structure (Figure 1) the ^{11}B spectrum consists of eight resonances of equal intensity (Table 4). The resonances arising from the six-boron subcluster are readily assigned by comparison with $[Pt_2(PMe_2Ph)_2(B_6H_9)_2]$.[9] Thus, that at $\delta(^{11}B)$ −42.9 is ascribed to B(1), and those at +12.1 and +6.9 p.p.m. to B(4) and B(5). Two of the three at $\delta(^{11}B)$ −2.4, −3.7, and −7.0 p.p.m., which all exhibit couplings to ^{195}Pt of around 300 Hz, consistent with direct linkages to the metal atom, are assigned to B(3) and B(6). These are those at −7.0 and −3.7 p.p.m. because that at −2.4 p.p.m. is assigned to B(8) by $^1H-\{^{11}B\}$ experiments (see below). Of the two resonances at low field, that at $\delta(^{11}B)$ +52.9 p.p.m. exhibits two different couplings $^1J(^{195}Pt-^{11}B)$ of *ca.* 560 and 240 Hz, and is therefore assigned to the more asymmetric B(7) position. That at +58.7 p.p.m., with fine structure interpretable in terms of two more nearly identical couplings $^1J(^{195}Pt-^{11}B)$ of *ca.* 330 Hz {*cf.* 330 ±20 Hz in $[Pt_2(PMe_2Ph)_2(B_6H_9)_2]$},[9] is assigned to B(2) which will be more equally bonded to the two different platinum atoms (see Figure 3).

The proton n.m.r. behaviour is of some importance, particularly in characterizing the novel two-boron subcluster, because hydrogen atoms were not located in the single-crystal *X*-ray diffraction analysis. Double resonance $^1H-\{^{11}B(selective)\}$ spectroscopy indicated nine hydrogen atoms for the six-boron subcluster and five for the two-boron subcluster. The terminal hydrogen atoms of the six-boron cluster were readily assigned as in Table 4, and three different B–H–B bridging hydrogen atoms were also apparent for this subcluster, the overall behaviour paralleling that of the $Pt_2B_6H_9$ units of $[Pt_2(PMe_2Ph)_2(B_6H_9)_2]$.[9]

Within the two-boron subcluster, selective irradiation of the low-field $^{11}B(7)$ resonance position in $^1H-\{^{11}B\}$ experiments indicated that this nucleus was coupled directly to protons at $\delta(^1H)$ +5.16, +2.65, and −0.28 p.p.m., and selective irradiation at the $^{11}B(8)$ resonance position indicated that this was also coupled directly to the proton at $\delta(^1H)$ +2.65 p.p.m., as well as to two others at +3.30 and +4.09 p.p.m. (Under the conditions that it was possible to carry out the experimentation any proton resonance fine structure arising from internuclear coupling, either to ^1H, ^{31}P, or ^{195}Pt, was unfortunately not discernible.)

Table 5. Proton and ^{31}P n.m.r. data for the phosphine ligands in $[Pt_2(PMe_2Ph)_2(B_2H_5)(B_6H_9)]$[a] and its proposed $(PPh_3)_2$ analogue[b]

	$[Pt_2(PMe_2Ph)_2(B_2H_5)(B_6H_9)]$[a]		$[Pt_2(PPh_3)_2(B_2H_5)(B_6H_9)]$[b]	
	A[c]	B[c]	C[c]	D[c]
$\delta(^{31}P)$/p.p.m.[d]	+3.8	−1.5	+44.2	+34.1
$^1J(^{195}Pt-^{31}P)$/Hz[e]	2 990	2 880	3 030	2 995
$^2J(^{195}Pt-^{31}P)$/Hz[c]	250	190	290	230
$^3J(^{31}P-^{31}P)$/Hz[f]	95		91	
$\delta(^1H)$/p.p.m.[g]	+2.15	+2.01	—	—
$^2J(^{31}P-^1H)$/Hz[h]	9.3	9.3	—	—
$^3J(^{195}Pt-^1H)$/Hz[h]	30.2	29.2	—	—

[a] This work; ^{31}P data in $CDCl_3$ solution at −50 °C; ^1H data in $CDCl_3$ solution at +21 °C. [b] Data from ref. 9; ^{31}P data in CD_2Cl_2 solution at −70 °C. [c] Inequivalent phosphine ligands. [d] ±0.5 p.p.m. [e] ±10 Hz. [f] ±2 Hz. [g] ±0.05 p.p.m. [h] ±0.5 Hz.

Table 6. Phosphine ligand n.m.r. parameters for the green compound of proposed formulation $[(PMe_2Ph)_3Pt_2B_9H_8(OMe)]$; CD_2Cl_2 solution[a]

	A[b]	B[b]	C[b]
$\delta(^{31}P)$/p.p.m.[c]	+2.1	−27.5	−37.1
$^1J(^{195}Pt-^{31}P)$/Hz[d]	3 142	2 422	*ca.* 2 990
$^2J(^{195}Pt-^{31}P)$/Hz[e]	273	10	8
$^3J(^{31}P-^{31}P)$/Hz[e]	11, 9[f]	11,[f] 27	9,[f] 27
$\delta(^1H)$/p.p.m.[g]	+2.25, +2.23	+1.59, +1.51, +1.46, +1.44	
$^2J(^{31}P-^1H)$/Hz	both *ca.* 10	all *ca.* 10	
$^3J(^{195}Pt-^1H)$/Hz	both *ca.* 30	*h*	

[a] ^{31}P Data at −50 °C; ^1H data at +21 °C. [b] Three inequivalent phosphine ligands; see structures (**12**), (**14**), and (**15**). [c] ±0.5 p.p.m. [d] ±10 Hz. [e] ±2 Hz. [f] 11 Hz splitting arises from $J(^{31}P_A-^{31}P_B)$; $J(^{31}P_A-^{31}P_C)$ appears to be somewhat smaller at *ca.* 9 Hz. [g] ±0.05 p.p.m. [h] ^{195}Pt satellites not well defined for the $Pt(PMe_2Ph)_2$ grouping, possibly due to ^{195}Pt chemical shift anisotropy relaxation (360 MHz spectrum).

The hydrogen atom with $\delta(^1H)$ +2.65 p.p.m. is ascribed to a B(7)–H–B(8) bridging position [structure (**8**)]. Although ostensibly at low field for bridging hydrogen it is associated with a low-field $^{11}B(7)$ resonance, and in a plot of $\delta(^1H)$ *versus* $\delta(^{11}B)$ [point (*a*), Figure 4] it does in fact appear some 2 p.p.m. above a line correlating the *exo*-hydrogen data, a feature diagnostic of B–H–B bridging hydrogen character.[15,17,19] The resonance at $\delta(^1H)$ −0.28 p.p.m., which was associated in $^1H-\{^{11}B\}$ experiments with only one boron nucleus, $^{11}B(7)$, is similarly ascribed to a B(7)–H–Pt(1) bridging position, because it is some 7 p.p.m. above the plot in Figure 4 [point (*b*)], diagnostic of B–H–M bridging behaviour.[15] (It is of interest in that a Pt–H–B bridging hydrogen atom is rare in polyhedral metallaborane and metallacarborane chemistry,[21] even though many platinaboranes[20,22,23] and platinacarboranes[24] have been reported.) The other three proton resonances in the two-boron subcluster are then reasonably assigned to the B-terminal positions, structure (**8**), other aspects of the shielding and $^1H-\{^{11}B\}$ double-resonance behaviour generally paralleling the corresponding behaviour[7,25–28] for other *arachno* four-vertex species [schematic structures (**9**)—(**11**)]. A particularly significant parallel concerns the magnitudes of the couplings $^1J(^{195}Pt-^{11}B)$ in $[Pt_2(PMe_2Ph)_2(B_2H_5)(B_6H_9)]$ and $[(PMe_2Ph)_2PtB_3H_7]$: in the $Pt_2B_2H_5$ subcluster (**8**) $^1J[^{195}Pt(2)-^{11}B(7)]$ is anomalously large at *ca.* 560 Hz, whereas $^1J[^{195}Pt(2)-^{11}B(8)]$ is smaller at *ca.* 330 Hz, paralleling the behaviour in $[(PMe_2Ph)_2PtB_3H_7]$ {schematic structure (**9**); $^1J[^{195}Pt(1)-^{11}B(3)]$ 565 Hz; $^1J[^{195}Pt(1)-^{11}B(2,4)]$ typical at *ca.* 300 Hz}.[15] This and the other n.m.r. parallels mentioned above confirm

Table 7. Proton and ^{11}B n.m.r. parameters for the cluster atoms of the green compound of proposed formulation $[(PMe_2Ph)_3Pt_2B_9H_8(OMe)]$; CD_2Cl_2 solution at +21 °C

$\delta(^{11}B)$/p.p.m.[a]	$\delta(^1H)$/p.p.m.[b]	Possible approx. couplings $^nJ(^{195}Pt-^1H)$/Hz
+91.4	+8.76	30
+43.1	+5.45	—
+38.8, +38.2 [c]	+6.47, +5.06 [c]	35, 30
+16.4[d]	*e*	—
+3.2	+16.4[e]	—
−6.8	+1.39[f]	—
−12.0, −12.5 [c]	+1.30[g]	—
	+2.94, +0.76 [h,i]	30, —

[a] $\delta(^{11}B)$ ±1.5 p.p.m.; all peaks in ^{11}B spectrum are doublets arising from $^1J(^{11}B-^1H)$ except resonance at $\delta(^{11}B)$ +21.0 p.p.m. (see footnote *d*). [b] $\delta(^1H)$ ±0.05 p.p.m. [c] ^1H Resonances too close for selectivity in $^1H-\{^{11}B\}$ decoupling experiments. [d] Singlet resonance, no coupling $^1J(^{11}B-^1H)$ apparent. [e] No directly bound *exo*-terminal H atom indicated; presumably OMe-substituted because ^1H spectrum exhibits $\delta(^1H)$ +3.32 p.p.m. (3 H), consistent with this. [f] Possible doublet splitting of 17 Hz. [g] Possible doublet splitting of *ca.* 13 Hz. [h] Possible doublet splitting of 31 Hz. [i] Possible doublet splitting of *ca.* 7 Hz.

that the four-vertex subcluster has *arachno* character as discussed above [see Figure 3(*b*) and (*c*)].

The $^{31}P-\{^1H(broad\text{-}band\ noise)\}$ n.m.r. spectrum, recorded at low temperatures to maximize 'thermal decoupling' of boron nuclei,[15,29] showed two different ^{31}P resonance centres and an essentially first-order analysis readily yielded the ^{31}P parameters summarized in Table 5, specific assignment of $^{31}P_A$ and $^{31}P_B$ between P(1) and P(2) not being critical because their n.m.r. parameters are so similar. Also in Table 5 are corresponding parameters for a recently reported product of the reaction between $[PtCl_2(PPh_3)_2]$ and 6,6′-$(B_{10}H_{13})_2O$,[9] the similarity suggesting that this may be a $(PPh_3)_2$ analogue of $[Pt_2(PMe_2Ph)_2(B_2H_5)(B_6H_9)]$.

(*iv*) *The proposed closed bimetallic cluster compound* $[(PMe_2Ph)_3Pt_2B_9H_8(OMe)]$. The n.m.r. results (Tables 6 and 7) constitute the bulk of the evidence for the nature of this air-stable green compound, isolated as an occasional product from the reaction between $[PtCl_2(PMe_2Ph)_2]$ and $(OMe)(SMe_2)B_9H_{12}$. The phosphine ligand data (Table 6) show that there are three platinum-bound phosphine ligands (none directly bound to boron), the various couplings $^2J(^{195}Pt-^{31}P)$ suggesting a system as in (**12**) in which phosphine A is bound transoid to Pt_B, and phosphines B and C are both cisoid to Pt_A. The magnitudes [15,20] of $^1J(^{195}Pt-^{31}P)$ suggest that both platinum atoms

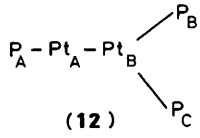

(**12**)

are bound contiguously in the polyhedral cluster, and the ^{11}B and ^1H data (Table 7) show nine different boron atoms, eight bound to *exo*-terminal hydrogen (see also Figure 4), with the ninth probably methoxy-substituted (see footnote *e* in Table 7). No bridging hydrogen atoms appear to be present. These considerations result in the formulation $[(PMe_2Ph)_3Pt_2B_9H_8(OMe)]$, implying an eleven-vertex Pt_2B_9 *closo*-type configuration, although any extensive two-orbital, or three-orbital 'T-shaped', cluster bonding participation by platinum

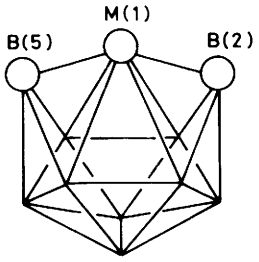

(13)

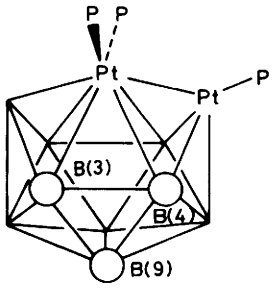

(14)

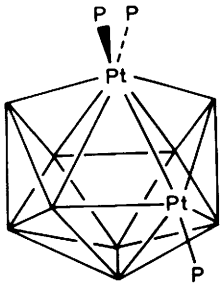

(15)

could induce more open structural features.[17,20,23] Here the (apparently) higher ^1H shieldings of three of the BH groupings [data (c) in Figure 4] could perhaps imply deviations from a straightforward closed cluster type, although their positions in this plot may merely reflect a different $\delta(^{11}B):\delta(^1H)(exo)$ correlation slope (*ca.* 12:1) for this species (*cf.* ref. 27).

A *closo* structure based on $[B_{11}H_{11}]^{2-}$ would presumably have one metal centre (probably Pt_B) at the six-connected position, structures (**13**)—(**15**). Known metallaboranes of *closo*-type geometry (**13**) have extremely low-field ^{11}B resonances [$\delta(^{11}B)$ *ca.* +100 p.p.m.] for B(2) and B(5).[15,30–33] The green compound has only one such resonance, possibly suggesting a structure (**14**) in which $Pt_A(PMe_2Ph)$ replaces one of these positions and the methoxy group is bound to one of B(3), B(4), or B(9). However, the other known eleven-vertex *closo*-type monometallaboranes do not have straightforward cluster electronic structures,[31–33] and so the ^{11}B shielding parallels may not extend to this diplatinum species. Present evidence therefore cannot exclude a configuration (**15**) in which Pt_A takes an off-mirror-plane position, with the site of methoxy substitution unspecified. Unfortunately the compound was not consistently obtained, and was never in high yield; nor have we so far been able to induce a suitable form of crystallization for single-crystal *X*-ray diffraction analysis.

Mechanistic Pathways.—The 7-methoxy and 1-chloro substituents on the nine-vertex platinaborane products of the reactions of equations (3) and (4) give mechanistic information, in that they show that the metal has added to the B(4)B(5)B(6) edge of the *arachno* nine-vertex substrates [(**16**); numbered as the enantiomer of (**2**)] and that the opposing B(8) vertex has been eliminated [(**17**) and (**18**); equation (5), L = SMe_2, (X,Y) = (H, Cl) or (OMe, H)]. It is of interest that the reaction does not occur *via* attack at the B(6)B(7)B(8) position

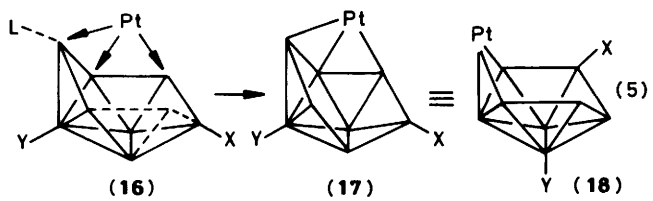

(16) (17) (18)

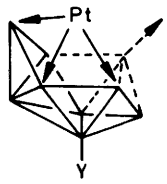

(19)

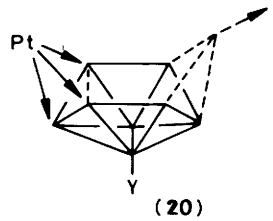

(20)

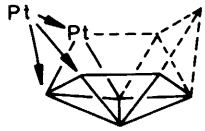

(21)

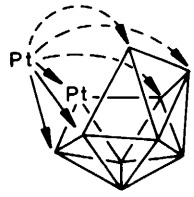

(22)

accompanied by elimination of the opposing B(4) vertex, because the latter could be regarded as already partially sequestered by the Lewis base SMe_2. Similar gross mechanisms could also account for the other species formed. Thus the formation of [2-Cl-4,4-$(PMe_2Ph)_2$-*arachno*-4-PtB_8H_{11}] from [3-Cl-*nido*-B_9H_{11}]$^-$ could involve attack by platinum at B(2)B(6)B(9) [*nido* nine-vertex numbering system as in (**3**)] and elimination of the opposing B(5) vertex as in (**19**), although attack at B(1)B(2)B(5) accompanied by opening of B(2)–B(5) and followed by elimination of the opposing B(9) vertex, structure (**20**), could also be envisaged.

Likewise a platinum centre adding at the Pt(4)B(5)B(6) edge of an initially formed *arachno*-4-platinaborane [numbering as in (**2**)], followed by loss, for example, of B(8) and B(9) [structure (**21**)] could occur in the formation of the Pt_2B_6 subclusters in $[Pt_2(PMe_2Ph)_2(B_6H_9)_2]$ and $[Pt_2(PMe_2Ph)_2(B_2H_5)(B_6H_9)]$; similarly an initial attack on an initially formed ten-vertex *arachno*-type intermediate [*e.g.* structure (**16**)], but now followed by cluster closure [structure (**22**)] rather than vertex loss, would account for the diplatinum *closo* structures postulated for $[(PMe_2Ph)_3Pt_2B_9H_8(OMe)]$. If this latter step was as in (**15**), however, then additional cluster rearrangement (*cf.* ref. 14) would have to be invoked.

Experimental

General and Nuclear Magnetic Resonance Spectra.—The starting metal complex $[PtCl_2(PMe_2Ph)_2]$ was prepared by standard methods.[9] Decaborane, $B_{10}H_{14}$, was obtained commercially and purified by sublimation before use, and $[NHEt_3][ClB_9H_{11}]$ was prepared from 1-Cl-4-(SMe_2)-*arachno*-B_9H_{12} (prepared as described below) by treatment with $[NHEt_3]OH$ as described in the literature;[34] the assignment of the chloro substituent to the 3-position in the $[ClB_9H_{11}]^-$ anion [structure (**3**) above] will be described elsewhere.[35] Other halogen-substituted nine- and ten-vertex borane species were prepared as described below. Reactions were generally carried out, and solutions and solids generally stored, under dry nitrogen, although manipulations and separatory procedures were generally carried out in air. Preparative t.l.c. was carried out using silica-gel G (Fluka, type GF 254, or Merck, type 60) on plates of dimensions 200 × 200 × 1 mm, made on glass formers from an acetone slurry followed by drying in air at 50—100 °C. N.m.r. spectroscopy at 2.35, 8.46, and 9.40 T was performed on JEOL FX-100 (at Leeds), Bruker WH 360 (S.E.R.C. service, University of Edinburgh), and Bruker WH-400 instruments (S.E.R.C. Service, University of Sheffield) respectively. The selective ^1H-$\{^{11}B\}$ experimental technique has been described elsewhere,[18,25,36,37] using the procedure in

which a ^1H-{^{11}B(off-resonance)} spectrum is subtracted from the ^1H-{^{11}B(on-resonance)} spectrum in order to remove lines arising from protons which are not coupled to the ^{11}B nucleus of interest.[10,29] Phosphorus-31 spectra were recorded at low temperatures to maximize 'thermal decoupling' of ^{10}B and ^{11}B, and thus reveal any coupling to other nuclei.[29] Other n.m.r. spectroscopy was straightforward. Chemical shifts $\delta(^1H)$, $\delta(^{31}P)$, and $\delta(^{11}B)$ are given in p.p.m. to high frequency (low field) of Ξ 100 (*i.e.* internal $SiMe_4$), Ξ 40.480 730 (nominally 85% H_3PO_4), and Ξ 32.083 971 MHz [nominally $BF_3(OEt_2)$ in $CDCl_3$][15] respectively.

Preparation of 2-X-6,9-$(SMe_2)_2$-$B_{10}H_{11}$ (X = Cl, Br, *or* I).[5]—In three separate experiments 2-$XB_{10}H_{13}$ (2 g) and Me_2S (10 cm^3) were stirred under N_2 at room temperature for 8 h. In each case a white crystalline solid was produced which was filtered and rapidly washed with hexane to give $Cl(SMe_2)_2$-$B_{10}H_{11}$, 3.3 g (93%) (Found: C, 16.9; H, 8.0. $C_4H_{23}B_{10}ClS_2$ requires C, 17.1; H, 8.2%); $Br(SMe_2)_2B_{10}H_{11}$, 2.8 g (85%);[5] $I(SMe_2)_2B_{10}H_{11}$, 2.6 g (87%) (Found: C, 14.0; H, 6.6; I, 32.2. $C_4H_{23}B_{10}IS_2$ requires C, 12.9; H, 6.2; I, 34.1%). Measured n.m.r. parameters are in Table 8.

Preparation of 4-(SMe_2)-7-(OR)-B_9H_{12} (R = Me *or* Et) *and* 1-X-4-(SMe_2)-B_9H_{12} (X = Cl, Br, *or* I).[5]—A freshly made sample of $Cl(SMe_2)_2B_{10}H_{11}$ (2 g) was heated in methanol or ethanol (50 cm^3) under reflux for 3 h. The solution was then allowed to cool to room temperature and the solvent removed under reduced pressure. The resulting yellow residue was dissolved in CH_2Cl_2 and separated by t.l.c. using a 1:1 mixture of CH_2Cl_2 and light petroleum (b.p. 40—60 °C). This produced two products, $Cl(SMe_2)B_9H_{12}$ (R_f 0.7) and $(SMe_2)(OMe)B_9H_{12}$ [or $(SMe_2)(OEt)B_9H_{12}$] (R_f 0.5), which were further purified by column chromatography using the same eluant to give, typically, 0.3 g (20%) of the chloro product and 0.4 g (28%) of the alkoxy product. Recrystallization of both products from CH_2Cl_2–light petroleum gave colourless needles. A similar method was used to prepare $Br(SMe_2)B_9H_{12}$ and $I(SMe_2)B_9H_{12}$ using the appropriate halogenated derivative $X(SMe_2)_2B_{10}H_{11}$ and in both cases a second product $(SMe_2)(OR)B_9H_{12}$ (R = Me or Et) was produced. Yields were similar to those given above. $Cl(SMe_2)B_9H_{12}$ (Found: C, 8.0; H, 10.9. $C_2H_{18}B_9ClS$ requires C, 8.8; H, 11.6%). (SMe_2)-$(OEt)B_9H_{12}$ (Found: C, 22.6; H, 10.7; B, 44.6. $C_4H_{23}B_9OS$ requires C, 22.0; H, 10.5; B, 45.4%). Measured n.m.r. parameters are in Table 9.

Reactions of Substituted arachno-*Nonaboranes with* $[PtCl_2(PMe_2Ph)_2]$.—In separate experiments 1-Cl-4-(SMe_2)-B_9H_{12} (1 mmol) or 4-(SMe_2)-7-(OMe)-B_9H_{12} (1 mmol) and 'proton sponge' (*N,N,N′,N′*-tetramethyl-1,8-diaminonaphthalene) (2 mmol) were stirred in benzene (20 cm^3) under N_2 for 30 min. A solution of $[PtCl_2(PMe_2Ph)_2]$ (1 mmol) in CH_2Cl_2 (20 cm^3) was added and the resulting solution was left stirring (2—3 h for reaction with the chloro derivative and 8 h for the methoxy derivative). The solvent was removed and the residue purified by t.l.c. using a 4:1 mixture of CH_2Cl_2 and light petroleum (b.p. 60—80 °C). The chloro derivative afforded a 30% yield of [2-Cl-4,4-$(PMe_2Ph)_2$-4-PtB_8H_{11}] (R_f 0.8). The methoxy derivative, after repeated purification by preparative t.l.c., afforded a 50% yield of [8-(OMe)-4,4-$(PMe_2Ph)_2$-4-PtB_8H_{11}] (R_f 0.4) together with several other products: (*i*) $[Pt_2(PMe_2Ph)_2(B_6H_9)_2]$, 35% yield, R_f 0.7; (*ii*) $[(PMe_2Ph)_2PtB_3H_7)]$, 8% yield, R_f 0.6; (*iii*) $[Pt_2(PMe_2Ph)_2(B_2H_5)(B_6H_9)]$, 1—2% yield, R_f 0.6; and (*iv*) $[(PMe_2Ph)_2Pt_2B_9H_8(OMe)]$, 0—2% yield, R_f 0.2. The mixture of compounds of R_f 0.6 [(*ii*) and (*iii*)] was heated in CH_2Cl_2 solution to 30 °C to degrade the compound from (*ii*), the process being monitored by n.m.r. spectroscopy. Repeated preparative-scale t.l.c. using a 3:7 mixture of CH_2Cl_2 and light petroleum (b.p. 60—80 °C) then afforded compound (*iii*). This was recrystallized from CH_2Cl_2–hexane to give air-stable yellow crystals. One such crystal (0.115 × 0.025 × 0.450 mm), free from flaws, was used for *X*-ray diffraction studies. The compound from (*iv*) crystallized from CH_2Cl_2–hexane as air-stable, dark green crystals which rapidly deformed *via* loss of solvent of crystallization.

Table 8. Boron-11 chemical shifts [$\delta(^{11}B)$/p.p.m.][a] for the substituted *arachno* ten-vertex species 2-X-6,9-$(SMe_2)_2$-$B_{10}H_{11}$ in $CDCl_3$ solution at +21 °C[b]

	X			
	H	Cl	Br	I
Assignment				
B(2)	−3.7	+7.2[c]	+0.9[c]	−0.5[c]
B(4)	−3.7	−4.4	−4.0	−3.8
B(5,7) and B(8,10)	−20.0[d]	−20.8[d]	−20.5[d]	−38.3[d]
B(6) and B(9)	−23.0[d]	−24.4[d]	−25.5[d]	−23.2, −28.6
E(1,3)	−40.1	−38.3	−38.3	−40.0

[a] $\delta(^{11}B)$ ± 1.5 p.p.m. relative to Ξ 32 083 971 Hz [nominally $BF_3(OEt_2)$ in $CDCl_3$]. [b] Data recorded at 32 MHz, all resonances are doublets due to $^1J(^{11}B–^1H)$, except where indicated. [c] Singlet resonance; no coupling $^1J(^{11}B–^1H)$ apparent. [d] Two near coincident resonance positions not resolved at 32 MHz.

Table 9. Proton and boron-11 nuclear shieldings[a] in substituted *arachno* nine-vertex species 4-(SMe_2)-B_9H_{12}X at +21 °C

	X = H[b,c]		X = 1-Cl[c]	X = 1-Br[c]	X = 7-(OMe)[c]	X = 7-(OEt)		
Assignment	$\delta(^{11}B)$[d]	$\delta(^1H)$[e]	$\delta(^{11}B)$[d]	$\delta(^{11}B)$[d]	$\delta(^{11}B)$[d]	$\delta(^{11}B)$ (C_6D_6)[d]	$\delta(^1H)$ ($CDCl_3$)[e]	$\delta(^1H)$ (C_6D_6)[e]
2, 3	−39.2	+0.44	−38.1	−38.1	−41.4	−40.9	+0.58	+1.29
4	−23.3	+0.39	*ca.* −22.4[f]	*ca.* −22.7[f]	−24.0	−22.5	+1.49	+0.38
6, 8	−21.5	+1.96, −0.01[g]	*ca.* −22.4[f]	*ca.* −22.7[f]	−21.9	−22.0	+1.49, +0.65[g]	+1.85, +1.78[g]
5, 9	−16.3	+1.81	−16.2	−16.4	−21.3	−23.6	+1.81	+2.37
1	+4.4	+3.04	+15.1[h]	+8.4[h]	+5.7	+6.3	+3.00	+3.34
7	+18.1	+4.07	+18.0	+18.2	+38.0[h]	+39.1[h]	—	—
(5,9), (6,8)[i]	—	−3.53	—	—	—	—	−3.11	−2.90
SMe_2	—	+2.54	—	—	—	—	+2.53	+1.35

[a] $\delta(^{11}B)$ in p.p.m. (±1.5) to high frequency (low field) of Ξ 32 083 971 Hz (ref. 15); $\delta(^1H)$ in p.p.m. (±0.05) to high frequency (low field) of internal $SiMe_4$; see also ref. 5. [b] See also ref. 19. [c] $CDCl_3$ solution. [d] All resonances are doublets due to $^1J(^{11}B–^1H)$ except where indicated by footnote *h*. [e] ^1H Resonances related to directly bound B positions by selective ^1H-{^{11}B} spectroscopy. [f] $^{11}B(4)$ and $^{11}B(6,8)$ resonance positions near coincident and not resolved in the 32 MHz spectroscopy used for these compounds. [g] *endo*-Terminal ^1H resonances. [h] Singlet resonance, no coupling $^1J(^{11}B–^1H)$ apparent. [i] Bridging ^1H resonances.

Table 10. Atom co-ordinates ($\times 10^4$) for $[Pt_2(PMe_2Ph)_2(B_2H_5)(B_6H_9)]$ with estimated standard deviations in parentheses

Atom	*x*	*y*	*z*	Atom	*x*	*y*	*z*
Pt(1)	−6 675.6(4)	−2 500	−3 233.0(11)	Me(21)	−9 069(12)	−732(18)	−2 637(37)
Pt(2)	−7 812.1(4)	−1 329.8(6)	−1 677.0(11)	Me(22)	−9 846(12)	−372(16)	−1 782(33)
P(1)	−5 611(2)	−3 395(3)	−4 614(7)	C(11)	−4 951(6)	−2 641(8)	−6 352(18)
P(2)	−8 803(2)	−334(3)	−216(7)	C(12)	−4 089(6)	−2 714(8)	−6 187(18)
B(1)	−8 374(16)	−3 934(22)	−1 512(41)	C(13)	−3 621(6)	−2 176(8)	−7 674(18)
B(2)	−7 583(13)	−2 914(18)	−826(38)	C(14)	−4 015(6)	−1 564(8)	−9 326(18)
B(3)	−7 310(13)	−3 910(19)	−2 664(38)	C(15)	−4 876(6)	−1 491(8)	−9 491(18)
B(4)	−8 253(17)	−4 289(23)	−4 390(45)	C(16)	−5 344(6)	−2 029(8)	−8 004(18)
B(5)	−9 063(18)	−3 509(25)	−3 595(48)	C(21)	−8 639(9)	1 015(8)	160(24)
B(6)	−8 688(13)	−2 656(18)	−1 382(36)	C(22)	−8 918(9)	1 696(8)	−1 507(24)
B(7)	−6 928(16)	−895(22)	−4 076(41)	C(23)	−8 760(9)	2 721(8)	−1 222(24)
B(8)	−7 048(13)	−073(19)	−1 835(39)	C(24)	−8 321(9)	3 064(8)	730(24)
Me(11)	−4 900(12)	−3 963(17)	−2 384(34)	C(25)	−8 041(9)	2 383(8)	2 398(24)
Me(12)	−5 892(12)	−4 478(18)	−6 417(35)	C(26)	−8 200(9)	1 358(8)	2 113(24)

Reaction between cis-$[PtCl_2(PMe_2Ph)_2]$ *and* $[NEt_4][nido\text{-}3\text{-}ClB_9H_{11}]$.—*cis-*$[PtCl_2(PMe_2Ph)_2]$ (0.54 g, 1.0 mmol) and a freshly made sample of $[NEt_4][3\text{-}ClB_9H_{11}]$ (0.2 g, 1.1 mmol) were dissolved in MeOH (*ca.* 10 cm^3) and stirred for 4 h. The solvent was evaporated (rotary evaporator) and the residue dissolved in a small volume of CH_2Cl_2 and applied to preparative t.l.c. plates. Development using an 80:20 mixture of CH_2Cl_2 and light petroleum (b.p. 60—80 °C) yielded $[2\text{-}Cl\text{-}4,4\text{-}(PMe_2Ph)_2\text{-}arachno\text{-}4\text{-}PtB_8H_{11}]$ (0.5 g, 0.8 mmol, 75%) as a yellow chromatographically mobile solid (R_f 0.8).

Crystallographic Studies on $[Pt_2(PMe_2Ph)_2(B_2H_5)(B_6H_9)]$.—All intensity data were recorded on a Syntex $P2_1$ diffractometer operating in the ω—2θ scan mode with graphite-monochromatized Mo-K_α radiation (λ = 71.069 pm). The cell dimensions, which were obtained by least-squares treatment of the setting angles of 15 reflections with $35 < 2\theta < 40°$, and the axial photographs showed the unit cell to be monoclinic. The systematic absences were $0k0$, $k = 2n + 1$ and the subsequent structure analysis was consistent with the space group $P2_1$ (no. 4). The 1 763 independent reflections with $4 < 2\theta < 45°$ were measured with scan speeds between 0.5 and 29° min^{-1}. Each scan speed ran from 1° below $K_{\alpha 1}$ to 1° above $K_{\alpha 2}$. Little, if any, decline in intensity of the check reflection (0,2,0) was observed during the course of the data collection. After correction for Lorentz, polarization, and transmission factors the 1 711 reflections with $I > 2\sigma(I)$ were retained for the structure analysis.

Solution and refinement of the structure. The two platinum atoms were located from a Patterson synthesis and the remaining atoms from difference syntheses. Full-matrix least-squares refinement with anisotropic thermal parameters for the platinum and phosphorus atoms and isotropic parameters for carbon and boron gave $R = 0.043$. Since the space group $P2_1$ is polar the structure of opposite polarity was also refined and gave $R = 0.040$. This was therefore taken to be the correct polarity. An attempt was made to locate the hydrogen atoms, but since not all those around the B_6 unit could be located with certainty, the peaks observed around the B_2 unit could not be relied upon. No hydrogen atoms were included in the final refinement. Least-squares weights were obtained from $w = 1/[\sigma^2(F_o) + 0.0004(F_o)^2]$ as carried out by the SHELX programs.[38] Final $R = 0.039$, $R' = 0.048$.

Crystal data for $[Pt_2(PMe_2Ph)_2(B_2H_5)(B_6H_9)]$. $C_{16}H_{36}B_8P_2Pt_2$, $M = 767.07$, monoclinic, $a = 1\,618.3(9)$, $b = 1\,330.0(7)$, $c = 592.3(3)$ pm, $\beta = 93.62(4)°$, $U = 1.272\,3(11)$ nm^3, space group $P2_1$, $Z = 2$, $D_c = 2.002$ g cm^{-3}, μ(Mo-K_α) = 112.24 cm^{-1}, $F(000) = 716$, 1 711 independent F_o with $I > 2\sigma(I)$. Final atomic co-ordinates are given in Table 10. An ORTEP drawing of the molecular structure is in Figure 1, and selected molecular dimensions are in Tables 1 and 2.

Acknowledgements

We thank the National University of Malaysia for sponsorship and the Department of Civil Service, Malaysia, for a grant (to R. A.), the S.E.R.C. for support, Dr. D. Reed (Edinburgh) for services in high-field n.m.r. spectroscopy, and Mr. A. Hedley for microanalysis.

References

1 Gmelin Handbuch der Anorganischen Chemie, Ergänzungswerk, Borverbindungen Teil 20, 1979, vol. 54.
2 N. N. Greenwood, in 'Comprehensive Inorganic Chemistry,' Pergamon Press, Oxford, 1973, ch. 11.
3 N. N. Greenwood and J. H. Morris, in 'Mellor's Comprehensive Treatise on Inorganic and Theoretical Chemistry,' Longman, London, 1981, Suppl. Vol. V, Part B1, Sect. B5.
4 T. L. Heying and C. Naar-Colin, *Inorg. Chem.*, 1964, **3**, 282.
5 B. Štíbr, J. Plešek, and S. Heřmánek, *Collect. Czech. Chem. Commun.*, 1969, **34**, 3241.
6 R. Ahmad, J. E. Crook, N. N. Greenwood, J. D. Kennedy, and W. S. McDonald, *J. Chem. Soc., Chem. Commun.*, 1982, 1019.
7 L. J. Guggenberger, A. R. Kane, and E. L. Muetterties, *J. Am. Chem. Soc.*, 1972, **94**, 5665.
8 N. N. Greenwood, M. J. Hails, J. D. Kennedy, and W. S. McDonald, *J. Chem. Soc., Chem. Commun.*, 1980, 37.
9 N. N. Greenwood, M. J. Hails, J. D. Kennedy,and W. S. McDonald, *J. Chem. Soc., Dalton Trans.*, 1985, 953.
10 S. K. Boocock, N. N. Greenwood, M. J. Hails, J. D. Kennedy, and W. S. McDonald, *J. Chem. Soc., Dalton Trans.*, 1981, 1415.
11 N. M. Boag, J. Browning, C. Crocker, P. L. Goggin, R. J. Goodfellow, M. Murray, and J. L. Spencer, *J. Chem. Res. (S)*, 1978, 228; C. E. Housecroft and T. P. Fehlner, *Inorg. Chem.*, 1982, **21**, 1739 and refs. therein.
12 D. E. Hyatt, F. R. Scholer, and L. J. Todd, *Inorg. Chem.*, 1966, **6**, 630.
13 R. F. Sprecher and J. C. Carter, *J. Am. Chem. Soc.*, 1973, **95**, 2369.
14 R. Ahmad, N. N. Greenwood, and J. D. Kennedy, unpublished work; see also, N. N. Greenwood, *Pure Appl. Chem.*, 1983, **55**, 1415.
15 J. D. Kennedy, 'Boron,' Chapter 8 in 'Multinuclear N.M.R. (N.M.R. in Inorganic and Organometallic Chemistry)', ed. J. Mason, Plenum, London and New York, in the press.
16 D. F. Gaines, C. K. Nelson, J. C. Kunz, J. H. Morris, and D. Reed, *Inorg. Chem.*, 1984, **23**, 3252.
17 M. A. Beckett, J. E. Crook, N. N. Greenwood, and J. D. Kennedy, *J. Chem. Soc., Dalton Trans.*, 1986, 1879.
18 T. C. Gibb and J. D. Kennedy, *J. Chem. Soc., Faraday Trans. 2*, 1982, 525.
19 J. E. Crook, N. N. Greenwood, J. D. Kennedy, and W. S. McDonald, *J. Chem. Soc., Dalton Trans.*, 1984, 2487.

20 J. D. Kennedy, *Prog. Inorg. Chem.*, 1984, **32**, 519; 1986, in the press.
21 R. N. Grimes, 'Boron Clusters with Metal-Hydrogen Bonds,' Chapter 7 in 'Metal Interactions with Boron Clusters,' ed. R. N. Grimes, Plenum, New York, 1982, pp. 269—319.
22 K. B. Gilbert, S. K. Boocock, and S. G. Shore, 'Compounds with Bonds between a Transition Metal and Boron,' Chapter 41.1 in 'Comprehensive Organometallic Chemistry,' eds. G. Wilkinson, F. G. A. Stone, and E. Abel, Pergamon, Oxford, 1982, vol. 6, pp. 879—945.
23 N. N. Greenwood, *Chem. Soc. Rev.*, 1984, **13**, 353.
24 R. N. Grimes, 'Metallacarboranes and Metallaboranes,' Chapter 5.5 in 'Comprehensive Organometallic Chemistry,' eds. G. Wilkinson, F. G. A. Stone, and E. Abel, Pergamon, Oxford, 1982, vol. 1, pp. 459—542.
25 J. Bould, N. N. Greenwood, J. D. Kennedy, and W. S. McDonald, *J. Chem. Soc., Dalton Trans.*, 1985, 1843.
26 J. Bould, N. N. Greenwood, and J. D. Kennedy, *J. Organomet. Chem.*, 1983, **249**, 11.
27 N. N. Greenwood, J. D. Kennedy, M. Thornton-Pett, and J. D. Woollins, *J. Chem. Soc., Dalton Trans.*, 1985, 2397.
28 R. C. Hopkins, J. D. Baldeschwieler, R. Schaeffer, F. N. Tebbe, and A. Norman, *J. Chem. Phys.*, 1965, **43**, 975.
29 J. D. Kennedy and J. Staves, *Z. Naturforsch., Teil B*, 1979, **34**, 808.
30 R. P. Micciche, J. J. Briguglio, and L. G. Sneddon, *Inorg. Chem.*, 1984, **23**, 3992.
31 J. E. Crook, M. Elrington, N. N. Greenwood, J. D. Kennedy, and J. D. Woollins, *Polyhedron*, 1984, **3**, 901.
32 J. E. Crook, M. Elrington, N. N. Greenwood, J. D. Kennedy, M. Thornton-Pett, and J. D. Woollins, *J. Chem. Soc., Dalton Trans.*, 1985, 2407.
33 H. Fowkes, N. N. Greenwood, J. D. Kennedy, and M. Thornton-Pett, *J. Chem. Soc., Dalton Trans.*, 1986, 517.
34 A. R. Siedle, G. M. Bodner, A. R. Garber, and L. J. Todd, *Inorg. Chem.*, 1977, **13**, 1756.
35 M. A. Beckett, M. Bown, X. L. R. Fontaine, N. N. Greenwood, J. D. Kennedy, and M. Thornton-Pett, unpublished work.
36 J. D. Kennedy and B. Wrackmeyer, *J. Magn. Reson.*, 1980, **38**, 529.
37 J. D. Kennedy and N. N. Greenwood, *Inorg. Chim. Acta*, 1980, **38**, 93.
38 G. M. Sheldrick, SHELX 76, Program System for *X*-Ray Structure Determination, University of Cambridge, 1976.

Received 9*th December* 1985; *Paper* 5/2150